Am J Transl Res 2026;18(8):6850-6865
www.ajtr.org /ISSN:1943-8141/AJTR0171012

Original Article

Polydatin ameliorates alcohol-induced gastric ulcer by inhibiting CASP3-mediated apoptosis

Lei Zhu, Yexin Tang, Qinglan Song, Yongbo Wang

Department of Gastroenterology, Taishun County People's Hospital, Wenzhou 325000, Zhejiang, China

Received December 25, 2025; Accepted June 4, 2026; Epub August 15, 2026; Published August 30, 2026

Abstract: Objective: To explore the protection of polydatin (PD) against alcoholic gastric ulcer (AIGU) in mice and the related molecular pathways. Methods: PD targets related to AIGU were predicted using network pharmacology, and Gene Ontology and Kyoto Encyclopedia of Genes and Genomes enrichment analyses were performed. A mouse gastric ulcer model was established via intragastric administration of ethanol, and the effects of PD on gastric mucosal morphology, oxidative damage, inflammation, and apoptosis-related proteins were evaluated; In vitro, the effects of PD on ethanol-injured GES-1 cells were further assessed in the presence or absence of the caspase-3 inhibitor Z-DEVD-FMK. Results: Network pharmacology showed that PD exerts its effects through apoptosis-related pathways. In vivo, PD significantly alleviated gastric mucosal injury, reduced the levels of malondialdehyde and pro-inflammatory cytokines, and increased the activities of antioxidant enzymes. It up-regulated mucosal protection factors (epidermal growth factor, prostaglandin E_2) and regulates apoptosis-related proteins (B-cell lymphoma-2, B-cell lymphoma-2-associated X protein, cysteinyl aspartate-specific proteinase-3). In vitro, PD protects gastric mucosal epithelial cells from apoptosis; the caspase-3 inhibitor Z-DEVD-FMK alone mimicked the protective effects of PD, and combined treatment with PD and Z-DEVD-FMK did not produce a markedly additive effect, suggesting that PD exerts its anti-apoptotic effect primarily through inhibition of caspase-3 (CASP3)-mediated apoptosis. Conclusion: PD exerts antioxidant, anti-inflammatory, and anti-apoptotic effects against AIGU, especially inhibiting CASP3-mediated apoptosis, which shows its potential as a natural gastric protection therapy.

Keywords: Polydatin, alcohol-induced gastric ulcer, CASP3, apoptosis, inflammation

Introduction

Gastric ulcers are a relatively common condition. They affect approximately 0.1% to 0.3% of people each year, thereby increasing the public health burden. Alcohol is a major risk factor for gastric mucosal injury; excessive alcohol consumption increases the risk of gastritis, gastric ulcer, and gastric cancer [1]. Alcohol damages the gastric mucosal barrier both directly and indirectly, such as decreasing bicarbonate or mucus secretion, triggering oxidative stress and apoptosis, and altering the permeability of mitochondrial membranes [2, 3]. These effects result in mucosal congestion, edema, epithelial cell loss, and mucosal erosion or ulceration [4-6]. Current treatments for alcohol-induced gastric ulcer (AIGU) mainly involve abstinence, nutritional support, and pharmacotherapies, such as acid-neutralizing agents, proton pump blockers, and histamine H2 receptor inhibitors. Although commonly prescribed, these therapies provide only limited clinical benefit, and their prolonged use may predispose patients to multiple adverse effects, ranging from ulcer relapse to hepatic and renal injury and cardiovascular complications [7, 8]. Therefore, the development of novel, more effective, and safer therapeutics for AIGU is of great clinical importance.

Traditional Chinese medicine regards gastric ulcer as primarily involving the stomach, often accompanied by liver and spleen dysfunction, and classifies it within the scope of "stomachache" syndromes caused by external pathogens, emotional disturbances, dietary irregularities, and spleen-stomach deficiency. Modern lifestyle factors, including excessive alcohol consumption and stress, exacerbate these pa-

https://doi.org/10.62347/ECGE1624

thogenic influences. Given their multitarget regulation and low side effects, the use of Chinese herbal medicines in the treatment of AIGU has received widespread attention. Polydatin (PD), a natural glycoside derived from *Polygonum cuspidatum*, exhibits antioxidant, anti-inflammatory, and anti-apoptosis activities [9, 10]. In addition, PD has shown protective effects in models of gastrointestinal diseases. Evidence suggests that PD exerts protective effects against DSS-induced colonic injury in experimental models of ulcerative colitis [9]. In addition, PD also has a protective effect on other models of gastrointestinal diseases, such as liver fibrosis and inflammatory bowel disease [11, 12]; this compound has therapeutic potential in disease models, but its specific role and molecular mechanism in AIGU remain unclear.

Caspases are key execution enzymes involved in the regulation of apoptosis. Cysteine aspartate protease 3 (CASP3) is a cysteine aspartic protease that plays a core role in apoptosis [13, 14]. CASP3 is typically activated by initiator caspases, such as CASP8 or CASP9 [15, 16]. The activated CASP3 can cleave substrates, such as poly (ADP-ribose) polymerase-1, Bax, and Bcl-2, which triggers the apoptotic cascade reaction. Dysregulation of CASP3 activity is associated with various pathological conditions, such as malignant tumors, age-related diseases, and cardiovascular diseases [17-19]. A 2023 study revealed that ethanol induces oxidative stress and mitochondrial damage in acute gastric mucosa injury and activates the endogenous apoptosis pathway and abnormal CASP3. Excessive CASP3 activity causes extensive apoptosis of gastric mucosal epithelial cells, destroys the integrity of the mucosal barrier, and aggravates ulcer formation [20]. Therefore, regulation of CASP3 activity is a promising method for the treatment of AIGU.

The protective role of PD in AIGU was systematically evaluated using animal and cell-based experimental models, with a focus on observing its regulation of CASP3-mediated apoptosis. In addition, we employed network pharmacology approaches to integrate multitarget prediction and pathway enrichment analyses, providing a holistic understanding of experimental evidence for the application of natural products in gastrointestinal diseases and provide novel insights and preventive and therapeutic strategies for AIGU.

Materials and methods

Network pharmacology

Identification of overlapping targets between PD and AIGU: Potential targets of PD were retrieved from the Traditional Chinese Medicine Systems Pharmacology (TCMSP) database, and a target interaction network for PD was established. The PD target network was visualized using Cytoscape software version 3.9.1. The keywords (e.g., ethanol-induced gastric ulcer) were searched in the GeneCards and Online Mendelian Inheritance in Man (OMIM) databases. After merging and removing duplicate genes, intersection targets between PD and AIGU were identified using an online bioinformatics platform, and a Venn diagram was generated.

Construction of the protein-protein interaction (PPI) network and Kyoto Encyclopedia of Genes and Genomes (KEGG) and Gene Ontology (GO) enrichment analyses: To build the core PPI network, we submitted the overlapping targets between PD and AIGU to the STRING database (http://string-db.org), applying a minimum confidence score cutoff of 0.400 and maintaining other parameters at default values. The constructed PPI network was subsequently visualized and analyzed for hub target identification using Cytoscape software version 3.9.1. GO and KEGG enrichment analyses were performed using R software: For GO analysis, the top 10 terms for biological process (BP), cellular component (CC), and molecular function (MF) were selected based on *P*-values and presented as combined bar charts. For KEGG pathway analysis, pathways with $P < 0.01$ were screened, and the top 20 with the smallest *P*-values were visualized.

Protein interaction analysis: Common targets were imported into Cytoscape to analyze protein-protein interactions and construct a protein interaction network of the shared targets.

Animal experimentation

Eight-week-old, female, specific-pathogen-free BALB/c mice weighing approximately 18.0 ± 2.0 g were obtained from Sibeifu Biotechnology Co., Ltd. (Beijing, China), under license number SCXK (Beijing) 2019-0010. They were housed at 22 ± 2°C and 50% ± 10% humidity under a

12 h light/dark cycle, with ad libitum access to food and water.

After acclimatization, the mice were randomly assigned to five groups (n = 5 per each): control (CON), model (MOD), low-dose PD (25 mg/kg), medium-dose PD (50 mg/kg), and high-dose PD (PD-H, 100 mg/kg) (SP8420, Solarbio, Beijing, China) groups. Throughout the experiment, all mice were provided with unrestricted access to standard feed and water. To minimize suffering during modeling and blood collection, mice were anesthetized with sodium pentobarbital (intraperitoneal injection, 40 mg/kg). PD or vehicle was administered orally once daily for 14 consecutive days, at a gavage volume of 10 mL/kg. Food was withheld for 22 h and water for 4 h prior to the final gavage.

Except for the CON group, the remaining groups received 75% ethanol (10 mL/kg) via oral gavage 1 h after the last treatment to induce AIGU [21]. At 1 h after ethanol administration, the mice were euthanized via intraperitoneal injection of an overdose of sodium pentobarbital (150 mg/kg). Blood was drawn from the orbital sinus, and the resulting serum was preserved at -20°C for subsequent examination. Following excision, the stomachs were longitudinally opened along the greater curvature. Tissue sections intended for histology were fixed in 10% neutral formalin, and the remaining samples were rinsed with saline, immediately frozen in liquid nitrogen, and stored at -80°C for molecular analysis.

Cell culture and treatment

Human gastric mucosal epithelial cells (GES-1) were obtained from Hefei Wanwu Biotechnology Co., Ltd. (Delf-10164). The cells were cultured in Roswell Park Memorial Institute 1640 medium supplemented with 10% fetal bovine serum (FBS, S9020, Solarbio, Beijing, China) and 0.5% penicillin/streptomycin (PB180120, Pricella, Wuhan, China) and incubated at 37°C under 5% CO_2 in a humidified environment.

The GES-1 cells were treated with ethanol (10, 20, 50, and 100 mmol/L) for 2 h to simulate ethanol-induced gastric epithelial cell injury in vitro. Detection of cell injury by cell viability assay: The ethanol concentration corresponding to approximately 60% cell viability is the optimal dose for modeling. For dose screening, cells were incubated with PD at various concentrations (10, 20, 40, 80, and 160 μM) for 24 h. Cell viability was measured to select non-toxic, protective concentrations for subsequent research.

Based on optimal model and intervention doses, the cells were divided into five groups: CON group, ethanol model group (MOD), PD-treated group (PD), CASP3 inhibitor group (Z-DEVD-FMK), and the combined PD and CASP3 inhibitor treatment group (PD + Z-DEVD-FMK). Z-DEVD-FMK (CM03299, Proteintech, Wuhan, China) was administered at 50 μM for 24 h pretreatment [22]. The PD, Z-DEVD-FMK, and combined treatment groups were then exposed to ethanol for 2 h to induce injury and intervention. Cells were collected for subsequent assays.

Hematoxylin and Eosin (H&E) staining

Gastric tissues embedded in paraffin were sliced into 4 μm-thick sections. Sections were deparaffinized in xylene I and II (5 min each) and rehydrated through graded ethanol. Then, staining was performed using the H&E kit (G1120, Solarbio, Beijing, China), as per the instructions provided by the manufacturer: staining with hematoxylin for 10 min, rinsing with PBS; differentiation in 10% acid alcohol for 3-5 s; rinsing again with PBS; staining with 1% eosin for 2 min, and final PBS wash. The sections were then dehydrated through graded ethanol, cleared, mounted with neutral resin, and observed under a light microscope.

Histopathological changes in gastric tissues were evaluated using a semiquantitative scoring system adapted from previous studies. Gastric mucosal injury was graded on a scale from 0 to 5, based on the severity of mucosal hyperemia, hemorrhage, epithelial cell degeneration, and glandular disruption [23]. All sections were analyzed in a blinded manner to reduce bias in scoring.

Measurement of epidermal growth factor (EGF) and prostaglandin E_2 (PGE_2)

Detection was performed using enzyme-linked immunosorbent assay (ELISA) kits (ml063178 for EGF, ml037542 for PGE_2; Suzhou Mlbio Company). In accordance with the instructions provided by the manufacturer, the content lev-

Table 1. Primers and probes for real-time qRT-PCR

Gene Name	Species	Sequence (5'-3')
TNF-α	Human	F: CTG AAC TTC GGG GTG ATC GG R: GGC TTG TCA CTC GAA TTT TGA GA
TNF-α	Mouse	F: CCCTGGTATGAGCCCATCTATC R: AAAGTAGACCTGCCCAGACTCG
IL-6	Human	F: AGACAGCCACTCACCTCTTCAG R: TTCTGCCAGTGCCTCTTTGCTG
IL-6	Mouse	F: TACCACTTCACAAGTCGGAGGC R: CTGCAAGTGCATCATCGTTGTTC
IL-1β	Human	F: CCAGGGACAGGATATGGAGCA R: TTCAACACGCAGGACAGGTACAG
IL-1β	Mouse	F: ATGATGGCTTATTACAGTGGCAA R: GTCGGAGTTCGTAGCTGGA
GAPDH	Human	F: GTCTCCTCTGACTTCAACAGCG R: ACCACCCTGTTGCTGTAGCCAA
GAPDH	Mouse	F: CATCACTGCCACCCAGAAGACTG R: ATGCCAGTGAGCTTCCCGTTCAG

Abbreviations: TNF-α, tumor necrosis factor-alpha; IL-6, interleukin-6; IL-1β, interleukin-1 beta; *GAPDH*, glyceraldehyde-3-phosphate dehydrogenase.

els of PGE_2 in the supernatant of mouse gastric tissue homogenate were detected. Absorbance was measured at 450 nm using a microplate reader (Varioskan LUX, Thermo Scientific, Waltham, USA), and concentrations were calculated accordingly.

Cell viability assay

Cell viability was assessed using a 3-(4,5-dimethylthiazol-2-yl)-2,5-diphenyltetrazolium bromide (MTT) assay kit (M1020, Solarbio, Beijing, China). Posttreatment, the cells were maintained in 100 μL MTT solution at 37°C for 1 h under dark conditions. After removal of the supernatant, 100 μL dimethyl sulfoxide was added to dissolve the formazan crystals with gentle shaking for 10 min. Absorbance was measured at 450 nm using a microplate reader (Varioskan LUX, Thermo Scientific, USA).

Oxidative stress and inflammatory marker assays

Serum from mice and supernatants from GES-1 cell cultures were collected after centrifugation. Malondialdehyde (MDA, A003-1-2), glutathione (GSH, A006-2-1), superoxide dismutase (SOD, A001-3-2), tumor necrosis factor-alpha (TNF-α, H052-1-2), interleukin-6 (IL-6, H007-1-2), and IL-1β (H002-1-2) levels were assessed with commercial kits obtained from Nanjing Jiancheng Bioengineering Institute. MDA, GSH, and SOD were determined via biochemical assays, and levels of TNF-α, IL-6, and IL-1β were assessed using ELISA, all following the manufacturers' protocols.

Terminal deoxynucleotidyl transferase dUTP nick end labeling (TUNEL) assay

Gastric tissues were fixed in 10% formalin, paraffin-embedded, and sectioned. TUNEL staining was conducted using a commercial kit (C1090, Beyotime, Shanghai, China), as per the manufacturer's protocol, to detect apoptosis. GES-1 cells were inoculated in 24-well plates, fixed, permeabilized, and stained similarly. After tissue sectioning and cell staining, fluorescence microscopy (Olympus BX53, Olympus, Tokyo, Japan) was performed for observation and imaging, and the proportion of apoptotic cells was analyzed.

Quantitative reverse transcription polymerase chain reaction (qRT-PCR)

Following the intervention, total RNA was isolated from murine gastric tissues utilizing an RNA extraction kit (R0017M, Beyotime, Shanghai, China). Analogously, total RNA was isolated from the treated GES-1 cells. RNA concentration and purity were assessed prior to reverse transcription into cDNA with the aid of a reverse transcription kit (RP1105, Solarbio, Beijing, China). Using the synthesized cDNA as a template, qRT-PCR was performed using a SYBR Green One-Step qRT-PCR kit (D7268S, Beyotime, Shanghai, China), in accordance with the manufacturer's instructions. Glyceraldehyde-3-phosphate dehydrogenase (GAPDH) was used as the internal reference gene, and the relative expression levels of target genes were calculated using the $2^{-\Delta\Delta Ct}$ method. Primer sequences are listed in **Table 1**.

Western blotting (WB)

After treatment, total protein was extracted from collected mouse gastric tissues and treated GES-1 cells by lysing them with radio-immu-

noprecipitation assay buffer (R0010, Solarbio, Beijing, China). Bicinchoninic acid assay (P00-12S, Beyotime, Shanghai, China) was used to measure protein concentrations. Sodium dodecyl sulfate-polyacrylamide gel electrophoresis (G2037-50T, Servicebio, Wuhan, China) was employed to separate equal amounts of protein, which were then transferred onto polyvinylidene difluoride membranes (P0021S, Beyotime, Shanghai, China). The membranes underwent blocking and were subsequently incubated with the following primary antibodies at 4°C overnight: Bax (60267-1-Ig, Proteintech, Wuhan, China), Bcl-2 (GB124830-100, Service bio, Wuhan, China), cleaved CASP3 (GB11532-100, Servicebio, Wuhan, China), CASP3 (19677-1-AP, Proteintech, Wuhan, China), and GAPDH (ml086777, Mlbio, Suzhou, China). After washing with tris-buffered saline containing Tween 20 (T1081, Solarbio, Beijing, China), the membranes were incubated with the appropriate horseradish peroxidase-conjugated secondary antibodies (GB23404, Servicebio, Wuhan, China), with GAPDH serving as the loading control. Enhanced chemiluminescence reagent (P00-18S, Beyotime, Shanghai, China) was used to detect protein bands, which were then imaged with a chemiluminescence detection system and quantified through densitometric analysis using ImageJ software (Ver.1.52b, NIH, Bethesda, MD, USA).

Statistical analysis

Statistical analysis was conducted using GraphPad Prism (v9.5, GraphPad Software, La Jolla, CA, USA). Results are expressed as mean ± standard deviation (SD). For comparisons between two groups, Student's t-test was applied, whereas multiple group differences were evaluated using one-way analysis of variance followed by Tukey's post hoc analysis. A P value < 0.05 was regarded as statistically significant.

Results

Network pharmacology analysis

Figure 1A shows that 193 PD-related targets were identified from the TCMSP, and 402 AIGU-associated targets were acquired from the OMIM database. After the integration and identification of intersection targets via the bioinformatics platform, 34 common targets between PD and alcohol-induced gastric ulcers were identified and visualized using a Venn diagram. The shared targets were uploaded to STRING database to construct the "PD-AIGU" PPI network, which was further visualized using Cytoscape 3.9.1 (**Figure 1B**). Circular nodes represent protein targets, where darker color and large node size indicating higher degree values.

GO enrichment analysis results (**Figure 1C**) reveal significant enrichment of these genes in BP, CC, and MF. In BP, the genes were mainly involved in responses to cytokines and regulation of apoptosis; in CC, they were enriched in extracellular regions and membranes; in MF, the genes were associated with protein binding and cytokine activity. KEGG pathway analysis identified significant enrichment in multiple signaling pathways, especially the top 20 pathways, including the TNF signaling pathway, which indicates that these signaling pathways can be critically involved in relevant physiological or disease-related processes (**Figure 1D**). Drug-target-pathway interactions were visualized in Cytoscape 3.9.1 (**Figure 1E**).

PD reduces oxidative damage and inhibits inflammation in AIGU mice

Compared with the CON, the MOD group showed a significant rise in serum MDA ($P < 0.01$) and marked decreases in GSH and SOD levels ($P < 0.001$). Moreover, ethanol exposure resulted in pronounced increases in pro-inflammatory cytokines, including TNF-α, IL-6, and IL-1β ($P < 0.001$) (**Figure 2A** and **2B**), which reflects the induction of oxidative stress and inflammatory responses. PD intervention improved these indicators in a dose-dependent manner. PD-H produced the most pronounced improvement. Notably, the MDA level decreased, GSH and SOD activities recovered, and the levels of pro-inflammatory cytokines decreased ($P < 0.05$ or $P < 0.001$) (**Figure 2A** and **2B**). qRT-PCR revealed that the mRNA levels of TNF-α, IL-6, and IL-1β in the gastric tissue of the MOD group were higher than those of the CON group ($P < 0.001$). PD treatment significantly reduced the expression levels of these genes, showing a dose-dependent characteristic. The inhibitory effect of the PD-H group was the most evident ($P < 0.05$ or $P < 0.001$) (**Figure 2C**). PD alleviated ethanol-induced gastric ulcers by reducing oxidative stress and inflammation in a dose-dependent manner.

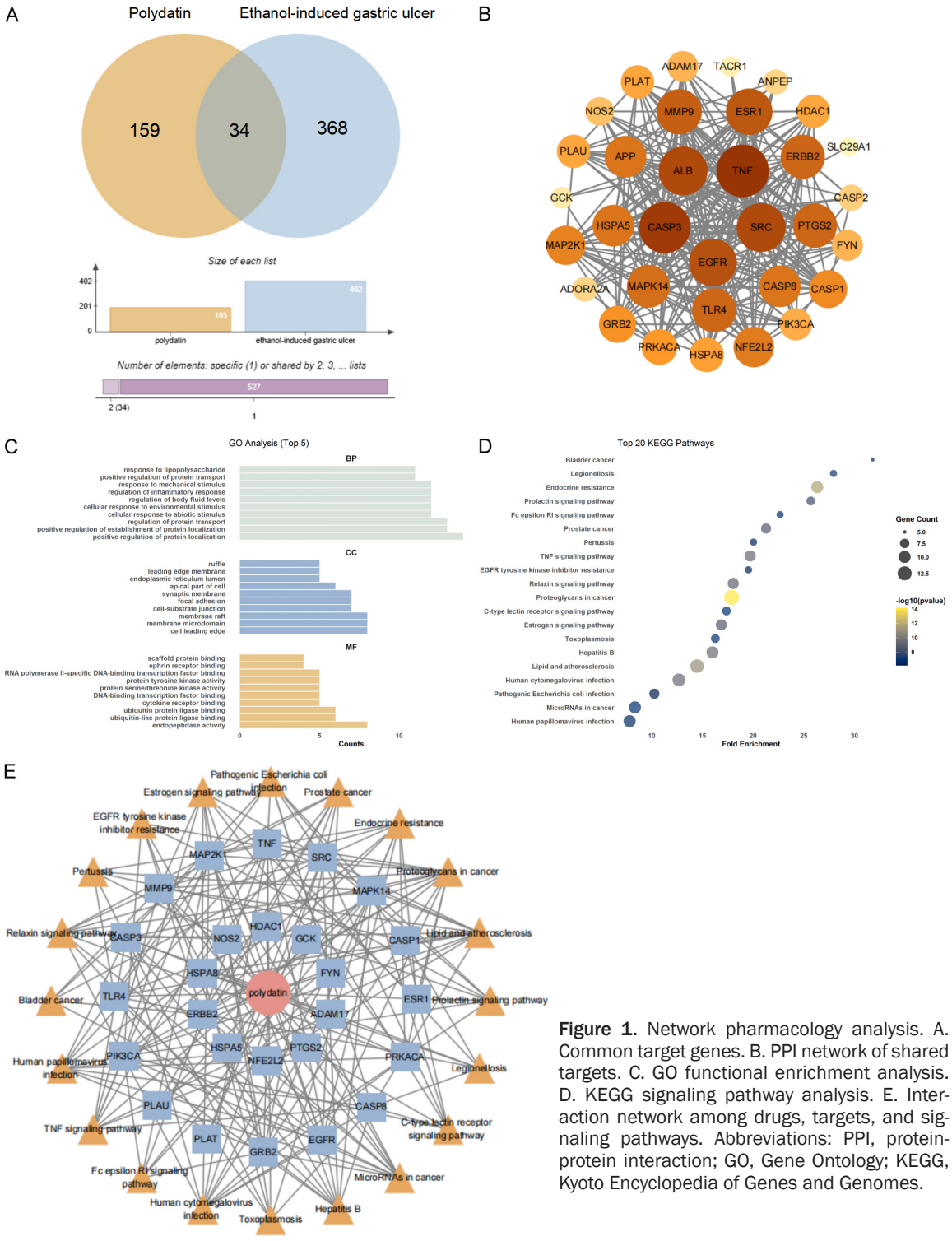

Figure 1. Network pharmacology analysis. A. Common target genes. B. PPI network of shared targets. C. GO functional enrichment analysis. D. KEGG signaling pathway analysis. E. Interaction network among drugs, targets, and signaling pathways. Abbreviations: PPI, protein-protein interaction; GO, Gene Ontology; KEGG, Kyoto Encyclopedia of Genes and Genomes.

PD modulates key factors and morphological changes in gastric tissues of mice with AIGU

Compared with the CON group, the levels of EGF and PGE_2 in the gastric tissue homogenate of the MOD group were significantly decreased ($P < 0.001$) (**Figure 3A**), which indicates that ethanol-induced gastric ulcer reduced the expression of gastric mucosal protection and repair factors. After PD treatment at different doses, the levels of EGF and PGE_2 increased significantly at large doses, with the PD-H group showing the most prominent increase ($P < 0.05$ or $P < 0.001$). This finding suggests that PD

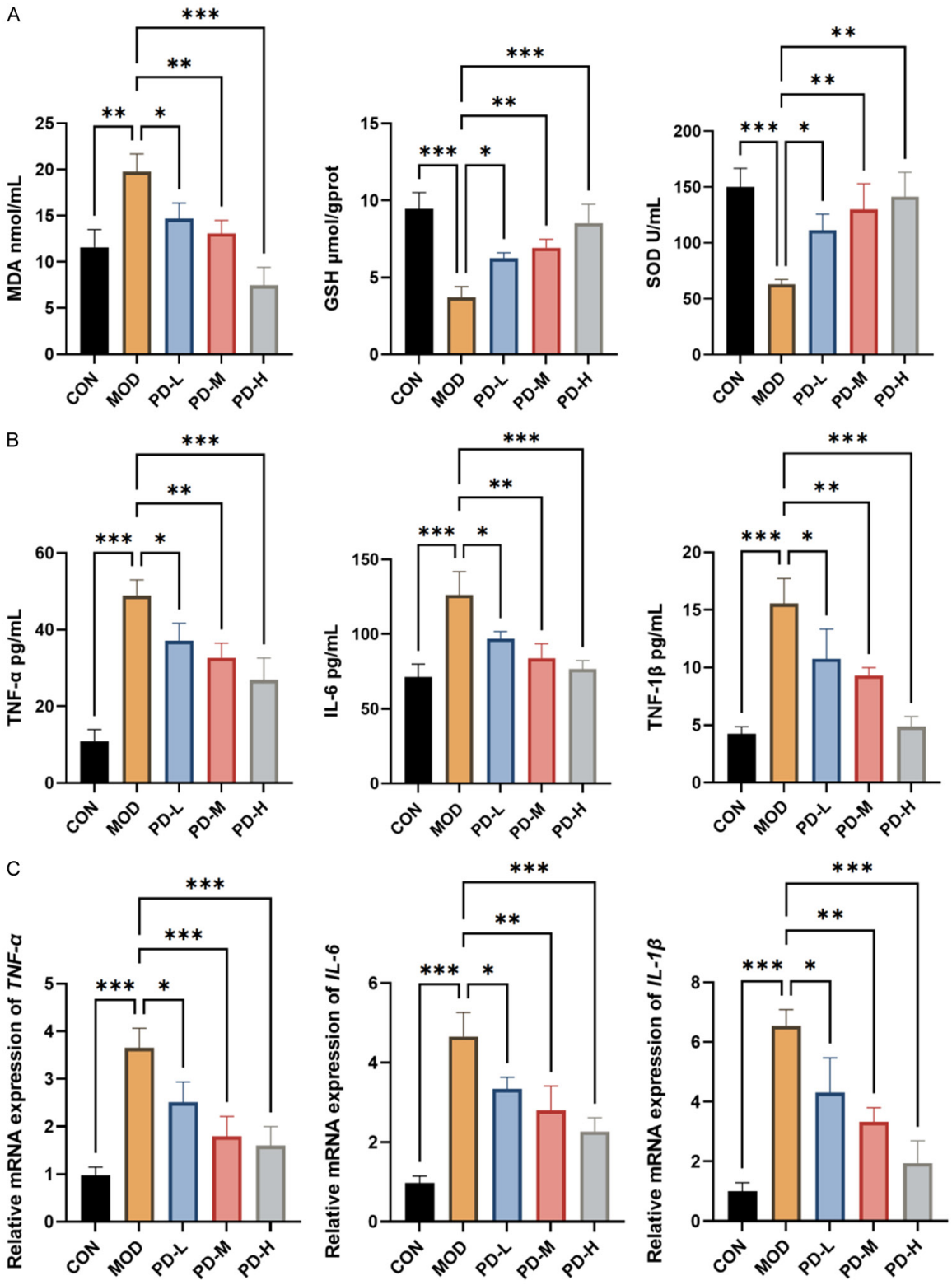

Figure 2. Impact of PD on oxidative stress and inflammatory markers in AIGU mice. A. Levels of MDA, GSH, and SOD activity in mouse serum. B. Serum levels of TNF-α, IL-6, and IL-1β. C. RT-qPCR analysis showing mRNA expression of *TNF-α*, *IL-6*, and *IL-1β* in gastric tissues. n = 5, *P < 0.05, **P < 0.01, ***P < 0.001. Abbreviations: PD, polydatin; AIGU, alcohol-induced gastric ulcer; MDA, malondialdehyde; GSH, glutathione; SOD, superoxide dismutase; TNF-α, tumor necrosis factor-alpha; IL-6, interleukin-6; IL-1β, interleukin-1 beta.

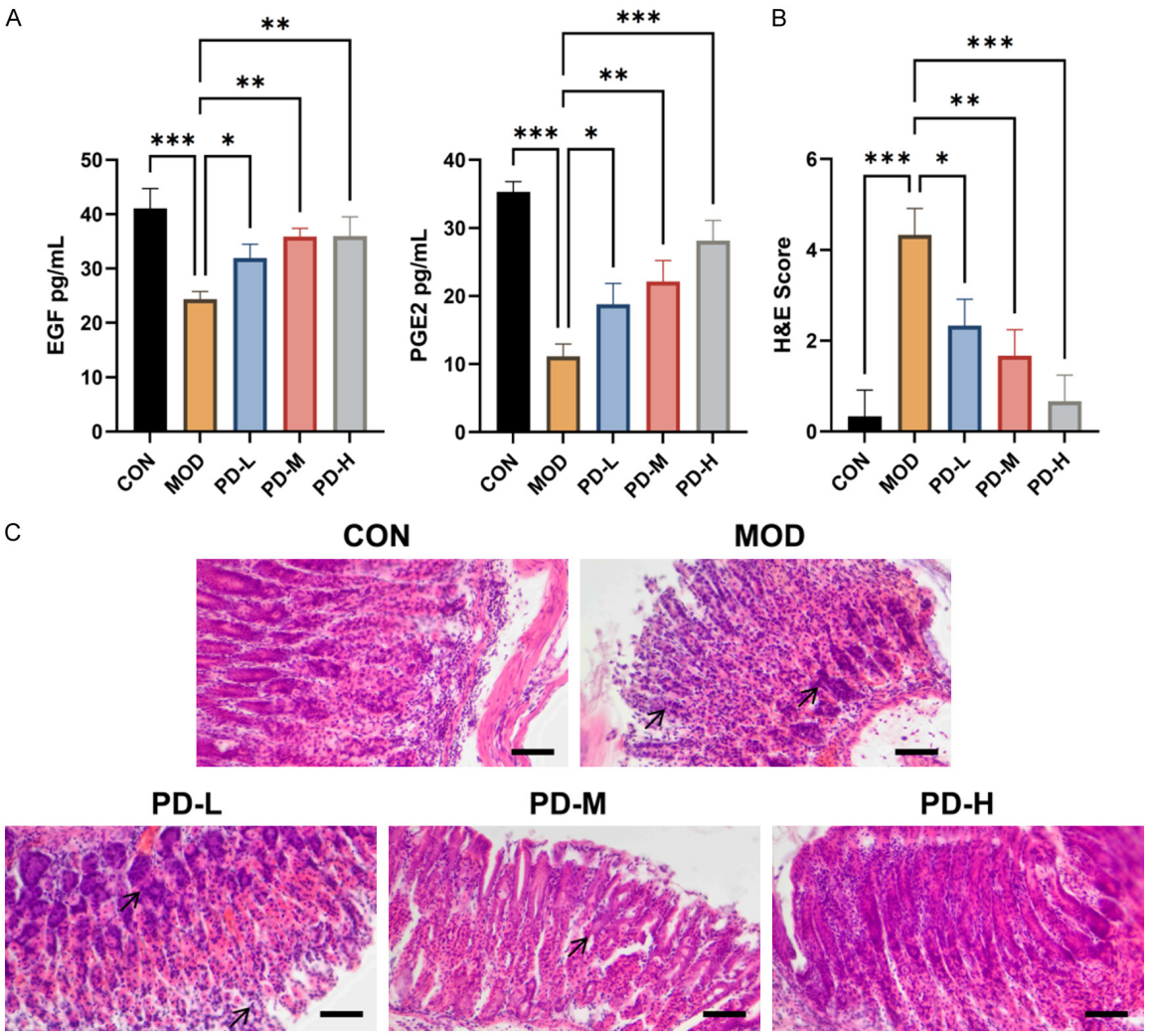

Figure 3. Effects of PD on gastric damage in AIGU mice. A. Quantification of EGF and PGE_2 concentrations in gastric tissue homogenates. B. H&E score. C. H&E staining of gastric tissue (×100, scale bar = 100 μm). n = 5, *P < 0.05, **P < 0.01, ***P < 0.001. Arrows indicate inflammatory cell infiltration and disorganization of tissue architecture. Abbreviations: PD, polydatin; EGF, epidermal growth factor; PGE_2, prostaglandin E_2.

may play a role by strengthening the self-repair of the gastric mucosa (**Figure 3A**). In H&E staining histological examination, the gastric mucosal structure of the CON group was intact without any pathological changes. The MOD group displayed the opposite, with typical ulcer lesions, such as epithelial shedding, gland destruction, and evident inflammatory cell infiltration. PD treatment gradually alleviated the pathological changes, especially in the PD-H group. The mucosal structure mostly recovered, the gland structure was orderly, and inflammatory infiltration was significantly reduced (**Figure 3B** and **3C**). These findings indicate that PD improves gastric mucosal injury and promotes tissue repair in AIGU mice by increasing the expressions of EGF and PGE_2.

PD attenuates gastric mucosal cell apoptosis in AIGU mice via regulation of apoptosis-related proteins

TUNEL analysis indicated that ethanol exposure led to an elevation in the number of apoptotic cells in the gastric mucosa of the MOD group compared with the controls (P < 0.001), which indicates that ethanol can induce apoptosis of gastric epithelial cells. PD administration dose-dependently reduced the number of apoptotic cells (P < 0.001), with the highest

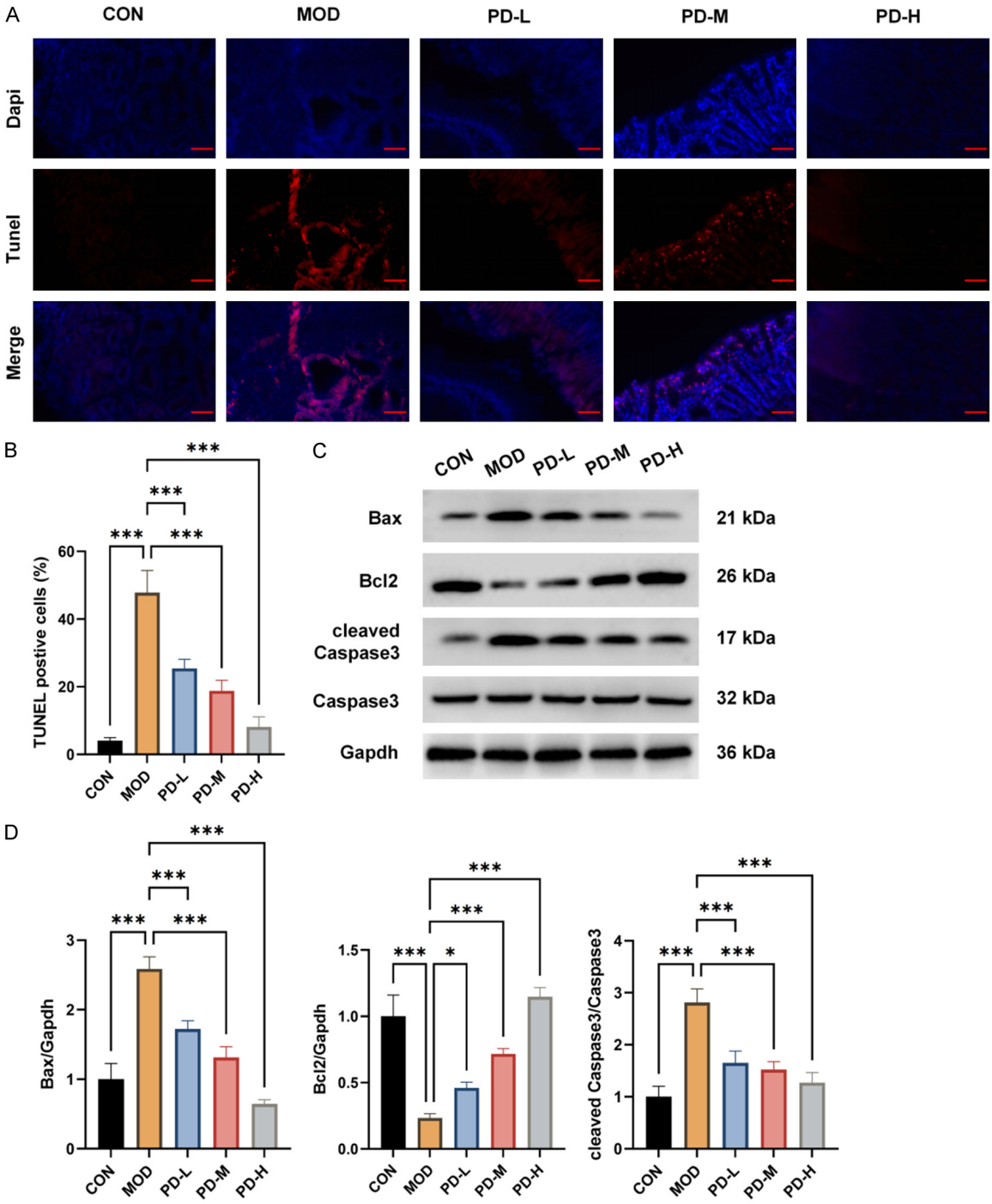

Figure 4. Impact of PD on apoptosis-associated indicators in gastric tissues from AIGU mice. A. TUNEL staining (×200, scale bar = 50 μm). B. Measurement of TUNEL-positive cell counts. C. Detection of apoptosis-related protein levels in gastric tissues using WB. D. Analysis of the relative expression levels of apoptosis-related proteins. n = 5, *P < 0.05, **P < 0.01, ***P < 0.001. Abbreviations: PD, polydatin; TUNEL, terminal deoxynucleotidyl transferase dUTP nick end labeling.

dose showing the strongest anti-apoptotic effect (**Figure 4A** and **4B**).

A significant increase in Bax and cleaved CASP3 expressions, along with a decrease in Bcl-2 level, was observed in the MOD group compared with the CON group (P < 0.001), as shown by WB. This finding suggests that ethanol induced activation of the gastric apoptotic pathway. PD treatment inhibited pro-apoptotic Bax

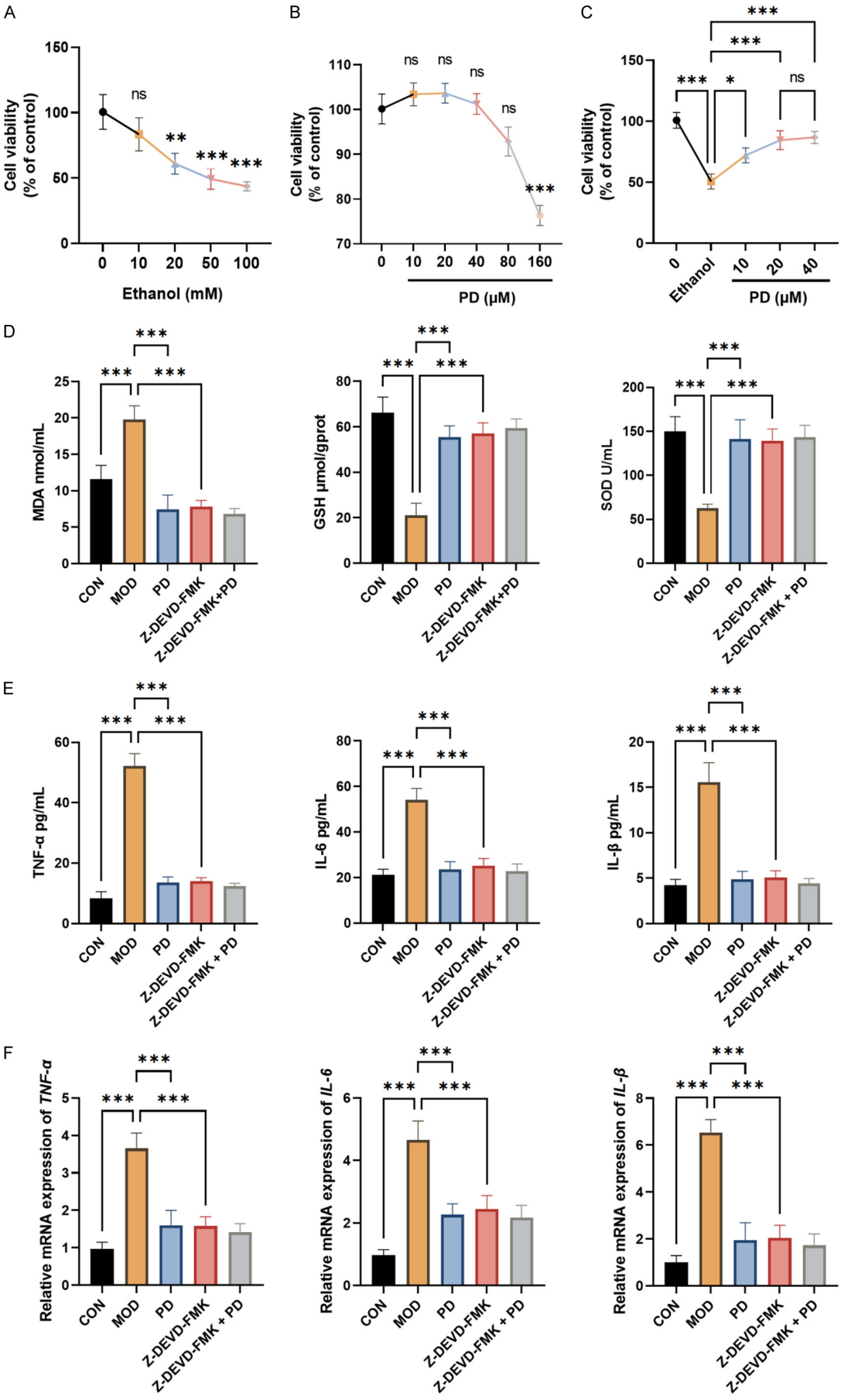
A
Cell viability (% of control)
Ethanol (mM)
0 10 20 50 100
ns
**
***
***
B
Cell viability (% of control)
PD (μM)
0 10 20 40 80 160
ns
ns
ns
ns
***
C
Cell viability (% of control)
0 Ethanol 10 20 40
PD (μM)
***
***
***
*
ns
D
MDA nmol/mL
GSH μmol/gprot
SOD U/mL
CON
MOD
PD
Z-DEVD-FMK
Z-DEVD-FMK+PD
Z-DEVD-FMK + PD
E
TNF-α pg/mL
IL-6 pg/mL
IL-β pg/mL
F
Relative mRNA expression of TNF-α
Relative mRNA expression of IL-6
Relative mRNA expression of IL-β

Figure 5. PD-mediated protection against ethanol-induced injury and involvement of CASP3 in oxidative and inflammatory responses. A. Effect of various ethanol concentrations on cell viability. B. Influence of escalating PD doses on cellular viability. C. Effect of ethanol and PD on cell survival rate. D. Quantification of intracellular MDA and enzymatic activities of GSH and SOD. E. Measurement of TNF-α, IL-6, and IL-1β concentrations in culture supernatants. F. mRNA expression levels of TNF-α, IL-6, and IL-1β assessed by RT-qPCR. n = 3, ns P > 0.05, *P < 0.05, **P < 0.01, ***P < 0.001, ns indicates no significance. Abbreviations: PD, polydatin; MDA, malondialdehyde; GSH, glutathione; SOD, superoxide dismutase; TNF-α, tumor necrosis factor-alpha; IL-6, interleukin-6; IL-1β, interleukin-1 beta; ns, no significance.

and cleaved CASP3 in a dose-dependent manner and promoted Bcl-2 expression (P < 0.001), which means that PD can counteract the apoptotic signal induced by ethanol (**Figure 4C** and **4D**). These outcomes show that PD inhibited apoptosis by regulating apoptosis-related proteins and gene expression, thereby playing a role in protecting the gastric tissue of AIGU mice.

PD alleviates ethanol-induced oxidative stress and inflammatory responses in GES-1 cells by inhibiting CASP3 activation

An MTT assay was performed to evaluate cell viability. After GES-1 cells were exposed to various concentrations of ethanol for 2 h, their viability displayed a dose-dependent decrease. When treated with 50 mM ethanol, the cell viability decreased significantly, and thus, this concentration was selected for model construction (**Figure 5A**). PD showed no evident cytotoxicity on GES-1 cells. When PD-treated cells (10, 20, and 40 μM) were exposed to ethanol, cell viability increased significantly. The protective effects of 20 and 40 μM were roughly similar, and 20 μM was selected for subsequent experiments (**Figure 5B** and **5C**).

In the MOD group, MDA levels were significantly higher than those in the CON group (P < 0.001), and GSH and SOD activities were notably reduced (P < 0.001) (**Figure 5D**), indicating that ethanol exposure triggered oxidative stress. PD treatment significantly reduced MDA levels (P < 0.001) and restored the activities of GSH and SOD (P < 0.001). Importantly, CASP3 inhibition alone (Z-DEVD-FMK group) produced protective effects similar to those of PD, as evidenced by decreased MDA levels and increased GSH and SOD activities. Moreover, no significant additional effect was observed in the PD + Z-DEVD-FMK group compared with either single treatment (**Figure 5D**), suggesting that PD and CASP3 inhibition converge on the same oxidative stress-related pathway. Similarly, levels of TNF-α, IL-6, and IL-1β were significantly increased in the MOD group compared with the CON group (P < 0.001), whereas PD treatment markedly reduced these cytokines (P < 0.001). CASP3 inhibition alone also mimicked the anti-inflammatory effect of PD, and no obvious additional reduction was observed in the combined treatment group (**Figure 5E**). RT-qPCR results further confirmed these trends (**Figure 5F**). These findings suggest that PD protects GES-1 cells against ethanol-induced oxidative stress and inflammatory injury, at least in part through modulation of the CASP3-mediated apoptotic pathway.

PD attenuates ethanol-induced gastric epithelial injury by inhibiting CASP3-mediated apoptosis

TUNEL staining showed that ethanol exposure significantly increased apoptotic cell numbers in the MOD group compared with the CON group (P < 0.001), indicating evident apoptosis induction (**Figure 6A** and **6B**). PD treatment significantly reduced the number of TUNEL-positive cells (P < 0.001), demonstrating a strong anti-apoptotic effect. Importantly, CASP3 inhibition alone (Z-DEVD-FMK group) mimicked the protective effect of PD, resulting in a similar reduction in apoptotic cells. Moreover, no significant additional reduction was observed in the PD + Z-DEVD-FMK group compared with either single treatment, suggesting that PD and CASP3 inhibition act on the same apoptotic axis.

Compared with the CON group, the MOD gro up exhibited significantly increased Bax and cleaved caspase-3 expression (P < 0.001) and markedly decreased Bcl-2 expression (P < 0.001) (**Figure 6C** and **6D**). PD treatment reversed these changes, decreasing pro-apoptotic protein levels and increasing anti-apoptotic Bcl-2 expression (P < 0.001). Notably, Z-DEVD-FMK alone produced similar effects to PD, while the combination group showed no obvi-

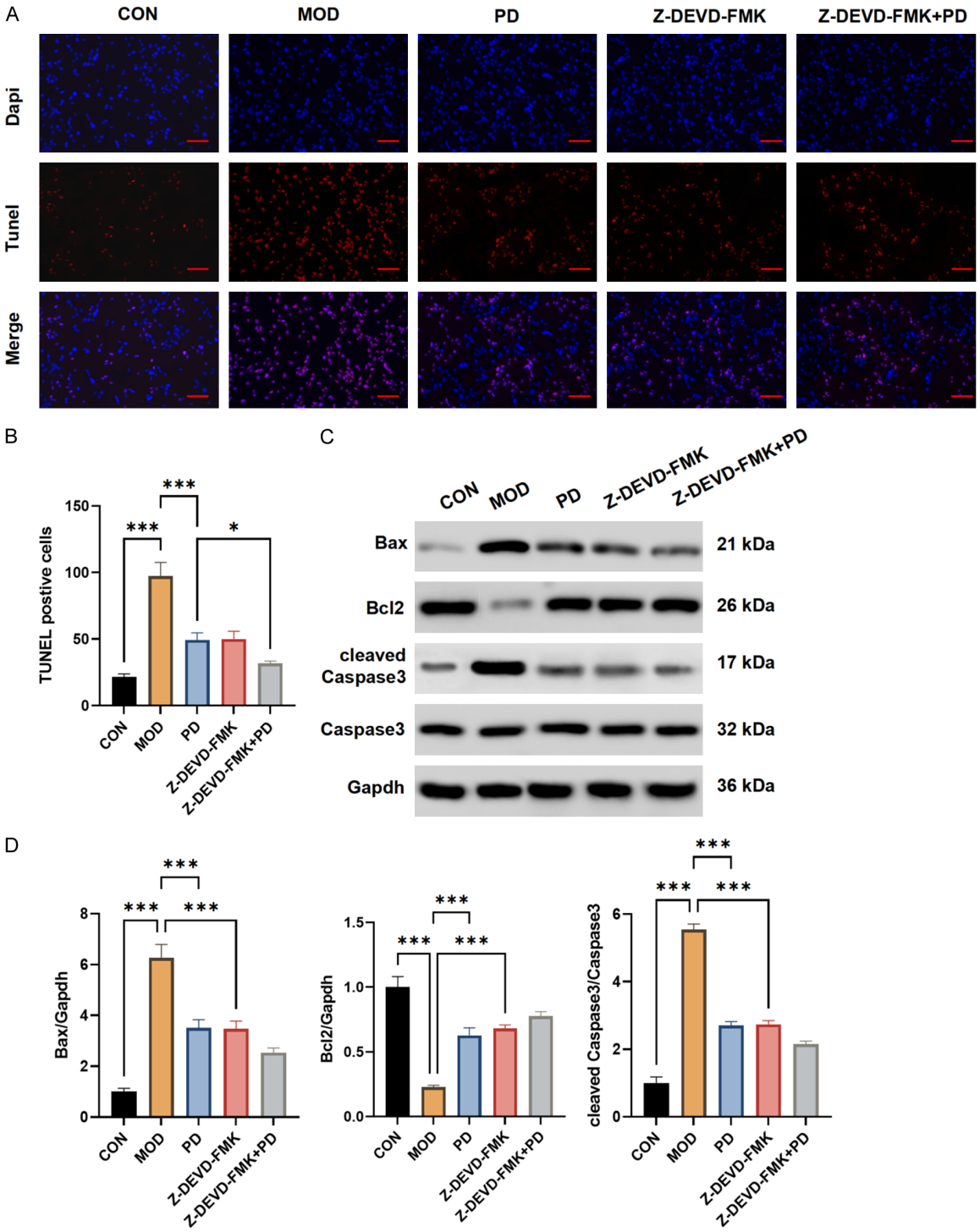

Figure 6. PD suppresses ethanol-triggered apoptosis via the modulation of the CASP3 pathway. A. TUNEL staining (×100, 100 μm). B. Quantification of TUNEL-positive cells. C. Detection of apoptosis-related protein levels in cells using WB. D. Examination of the relative protein expression levels involved in apoptosis. n = 3, ***P < 0.001, vs. MOD; *P < 0.05, **P < 0.01. Abbreviations: PD, polydatin; TUNEL, terminal deoxynucleotidyl transferase dUTP nick end labeling.

ous additive effect compared with either treatment alone. These results indicate that PD mitigates ethanol-induced gastric epithelial injury through regulation of apoptosis-associated proteins and suppression of the CASP3-dependent apoptotic cascade.

Discussion

Gastric ulcers are a prevalent disorder with diverse etiologies and a notably high incidence rate. Most current clinical therapies are associated with adverse effects, high recurrence rates, and prolonged treatment durations. Therefore, finding safe and effective anti-ulcer drugs from traditional Chinese medicine natural compounds has therapeutic potential [24]. PD is a naturally occurring polyphenol that exhibits pronounced antioxidant activity and notable anti-inflammatory effects [25]. In the present work, a network pharmacological approach was applied to identify 34 putative targets common to PD and AIGU. Subsequent GO and KEGG enrichment analyses showed that PD may play a role by regulating apoptosis, reducing oxidative stress, and modulating inflammatory pathways. These predictions were verified by experiments in vivo and in vitro.

Oxidative stress influences the pathogenesis of AIGU [26]. Ethanol produces a large amount of reactive oxygen species (ROS) during metabolism, such as superoxide anions and hydroxyl radicals. These ROS can initiate lipid peroxidation reactions, thereby destroying the structural organization of the stomach [27, 28]. MDA, as the end product of lipid peroxidation, can cause denaturation and deposition of proteins and nucleic acids, leading to cell damage [29]. This work revealed that PD treatment can reduce the level of MDA in gastric tissue and increase the activities of SOD and GSH, which indicates that it can enhance the antioxidant defense, inhibit lipid peroxidation, and reduce the tissue damage caused by oxidative stress. Similar effects were also observed in GES-1 cells in vitro. This finding is consistent with the research of Kan et al., who pointed out that natural products relieve gastric ulcers through antioxidant pathways [30].

The development of AIGU is driven by the inflammatory response, which involves a variety of pro-inflammatory cytokines. Growing studies suggest that dysregulated expression of cytokines, particularly TNF-α and IL-6, contribute substantially to the pathogenesis and progression of acute gastric ulcers. TNF-α significantly promotes neutrophil infiltration into the gastric mucosa, and IL-6 synergistically induces the expression of other pro-inflammatory mediators, thereby amplifying the inflammatory cascade [31, 32]. TNF-α can trigger the accumulation of neutrophils in the ulcer area, leading to local microcirculatory disorders and aggravating mucosal damage [33]. The histopathological examination of this study showed that the gastric mucosa in the MOD group was seriously damaged, the gland structure was destroyed, and evident congestion, edema and inflammatory cell infiltration occurred. After PD treatment, these pathological features were greatly relieved, the mucosal structure was relatively well maintained, and inflammatory infiltration was greatly reduced. PD intervention was associated with a substantial suppression of gastric TNF-α, IL-6, and IL-1β expressions, as evidenced by cytokine analysis. The results of RT-qPCR were consistent with those of ELISA detection, which confirmed that the levels of pro-inflammatory cytokines were decreased. When ethanol was used to treat GES-1 cells in vitro, PD had a similar anti-inflammatory activity. These findings indicate that PD can inhibit the production of pro-inflammatory cytokines, reduce mucosal inflammation, and protect the gastric mucosa. In general, these data indicate that PD has the potential to be a feasible therapy for gastric ulcers.

EGF and PGE_2 play critical roles in mucosal defense and repair. EGF can promote epithelial cell proliferation and repair, reduce gastric acid secretion, and increase the synthesis of glycoproteins [34]. PGE_2 can enhance mucosal blood flow, promote the migration and regeneration of epithelial cells, and maintain the integrity of the mucosal barrier [35]. Our results show that PD increased the concentrations of EGF and PGE_2. This compound possibly assists in the healing of ulcers by enhancing the regeneration of the mucosa and barrier functions.

A key factor in the occurrence and development of gastric mucosal injury is the imbalance of cell apoptosis. Under normal physiological conditions, the gastric mucosa relies on cell proliferation and programmed cell death [36] to maintain its balance of structure and function. However, harmful stimuli, especially ethanol, disrupt this balance, which causes increased cell apoptosis, damage to cell structure and dysfunction, and aggravated pathological changes in the gastric mucosa [23, 37, 38]. Ethanol challenge markedly promoted apoptosis in

gastric tissues and GES-1 cells, as evidenced by TUNEL staining. Ethanol challenge induced a shift in apoptosis-related protein expression, characterized by elevated Bax and cleaved CASP3 levels and suppressed Bcl-2 expression, as confirmed by RT-qPCR and WB, which ultimately contributed to gastric mucosal injury. PD intervention protects gastric mucosal cells by reducing Bax and cleaved CASP3, increasing Bcl-2, restoring the Bax/Bcl-2 ratio, and thereby inhibiting excessive apoptosis. To further clarify the involvement of CASP3 in the protective mechanism of PD, the caspase-3 inhibitor Z-DEVD-FMK was used as a functional validation strategy in vitro. CASP3 inhibition alone mimicked the anti-apoptotic effect of PD, and no obvious additional protective effect was observed when PD was combined with Z-DEVD-FMK, suggesting a functional convergence on the same apoptotic pathway. This outcome indicates that PD inhibits apoptosis through the CASP3 pathway, highlighting its protective effect.

In conclusion, PD is a natural multi-target agent. It alleviates alcohol-induced gastric ulcer through mechanisms such as antioxidant and anti-inflammatory effects, enhancement of mucosal repair, and inhibition of cell apoptosis. PD regulates apoptosis-related pathways, reduces the production of oxidative stress and inflammatory cytokines, promotes mucosal healing, and protects gastric epithelial cells. In vitro, CASP3 inhibition by Z-DEVD-FMK produced effects similar to those of PD, and their combined treatment did not show an obvious additive protective effect, suggesting that PD alleviates apoptosis mainly via the CASP3 pathway. Findings from this study provide strong experimental evidence for the advancement of PD as a natural, safe, and efficacious treatment option for gastric ulcers. Although these results are encouraging, certain limitations should be acknowledged: the study focused on acute ethanol-induced gastric injury in mice, which may not fully reflect chronic or multifactorial human ulcers, and the pharmacokinetics and safety profile of PD were not evaluated. Furthermore, although CASP3-mediated apoptosis was examined, other potential mechanisms remain unexplored. Future studies should investigate chronic ulcer models, clarify PD's pharmacological properties, and explore additional molecular targets to further validate its therapeutic potential.

Acknowledgements

This research was funded by the Science and Technology Program of Wenzhou (No. Y20240388).

Disclosure of conflict of interest

None.

Address correspondence to: Yongbo Wang, Department of Gastroenterology, Taishun County People's Hospital, No. 195, Xincheng Avenue, Taishun County, Wenzhou 325000, Zhejiang, China. Tel: +86-1395-8987980; E-mail: wyb_586318@163.com

References

[1] Salaheldin AT, Shehata MR, Sakr HI, Atia T and Mohamed AS. Therapeutic potency of ovothiol A on ethanol-induced gastric ulcers in Wistar rats. Mar Drugs 2022; 21: 25.

[2] Lu S, Kong S, Wang Y, Hu Z, Zhang L and Liao M. Gastric acid-response chitosan/alginate/tilapia collagen peptide composite hydrogel: protection effects on alcohol-induced gastric mucosal injury. Carbohydr Polym 2022; 277: 118816.

[3] Kim HR, Kim MC, Kang EJ, Choi JH, Choi YK, Lee IB, Choi DH, Seo YJ, Noh JR, Kim YH and Lee CH. The gastroprotective effect of *sicyos angulatus* against hydrochloric acid/ethanol-induced acute gastritis and gastric ulcer in mice. J Med Food 2024; 27: 1219-1230.

[4] Qin S, Huang K, Fang Z, Yin J and Dai R. The effect of Astragaloside IV on ethanol-induced gastric mucosal injury in rats: involvement of inflammation. Int Immunopharmacol 2017; 52: 211-217.

[5] Carneiro JG, Holanda TBL, Quinderé ALG, Frota AF, Soares VVM, Sousa RS, Carneiro MA, Martins DS, Gomes Duarte AS and Benevides NMB. Gastroprotective effects of sulphated polysaccharides from the alga caulerpa mexicana reducing ethanol-induced gastric damage. Pharmaceuticals (Basel) 2018; 11: 6.

[6] Yang J, Zhou W, Gu Y, Dai J, Li X, Tai P, Li Y, Ma X and Zhang Y. Protective effect of Pu-erh tea extracts against ethanol-induced gastric mucosal damage in rats. Biomed Rep 2018; 8: 335-342.

[7] Sánchez-Mendoza ME, López-Lorenzo Y, Cruz-Antonio L, Matus-Meza AS, Sánchez-Mendoza Y and Arrieta J. Gastroprotection of calein D against ethanol-induced gastric lesions in mice: role of prostaglandins, nitric oxide and sulfhydryls. Molecules 2019; 24: 622.

[8] Yang Y, Wang Z, Zhang L, Yin B, Lv L, He J, Chen Z, Wen X, Qiao B, Sun W, Fang M and Zhang Y.

Protective effect of gentiopicroside from Gentiana macrophylla Pall. in ethanol-induced gastric mucosal injury in mice. Phytother Res 2018; 32: 259-266.
[9] Chen G, Yang Z, Wen D, Guo J, Xiong Q, Li P, Zhao L, Wang J, Wu C and Dong L. Polydatin has anti-inflammatory and antioxidant effects in LPS-induced macrophages and improves DSS-induced mice colitis. Immun Inflamm Dis 2021; 9: 959-970.
[10] Sun Z and Wang X. Protective effects of polydatin on multiple organ ischemia-reperfusion injury. Bioorg Chem 2020; 94: 103485.
[11] Lan T, Zhuang L, Li S, Yang G, Xuan Y and Guo J. Polydatin attenuates hepatic stellate cell proliferation and liver fibrosis by suppressing sphingosine kinase 1. Biomed Pharmacother 2020; 130: 110586.
[12] Liu YJ, Xu WH, Fan LM, Zhang YQ, Xu W, Chen YP, Chen LL, Chen L, Xu W, Wang Y, Chu KD and Zhang JP. Polydatin alleviates DSS- and TNBS-induced colitis by suppressing Th17 cell differentiation via directly inhibiting STAT3. Phytother Res 2022; 36: 3662-3671.
[13] Liu X, Song X, Luan D, Hu B, Xu K and Tang B. Real-time in situ visualizing of the sequential activation of caspase cascade using a multicolor gold-selenium bonding fluorescent nanoprobe. Anal Chem 2019; 91: 5994-6002.
[14] Khezri MR, Ghasemnejad-Berenji M and Moloodsouri D. The PI3K/AKT signaling pathway and caspase-3 in Alzheimer's disease: which one is the beginner? J Alzheimers Dis 2023; 92: 391-393.
[15] Basu V, Shabnam, Murghai Y, Ali M, Sahu S, Verma BK and Seervi M. ONC212, alone or in synergistic conjunction with Navitoclax (ABT-263), promotes cancer cell apoptosis via unconventional mitochondrial-independent caspase-3 activation. Cell Commun Signal 2024; 22: 441.
[16] Chen L, Li X, Cheng M, Wang S, Zheng Q and Liu Q. Iso-pencillixanthone A from a marine-derived fungus reverses multidrug resistance in cervical cancer cells through down-regulating P-gp and re-activating apoptosis. RSC Adv 2018; 8: 41192-41206.
[17] Bhat AA, Thapa R, Afzal O, Agrawal N, Almalki WH, Kazmi I, Alzarea SI, Altamimi ASA, Prasher P, Singh SK, Dua K and Gupta G. The pyroptotic role of Caspase-3/GSDME signalling pathway among various cancer: a review. Int J Biol Macromol 2023; 242: 124832.
[18] Lee JC, Kim GC, Kim SW, Lee NK, Cho YS, Chung SW, Lee YS, Han MW, Chang HW, Byun Y and Kim SY. Letter-to-editor, "Feedback amplification of senolysis using caspase-cleavable peptide-doxorubicin conjugate and 2DG" [Journal of Controlled Release, Volume 346, pp. 158-168, (2022), doi: 10.1016/j.jconrel.2022.04.012]. J Control Release 2023; 362: 779-783.
[19] Ji N, Qi Z, Wang Y, Yang X, Yan Z, Li M, Ge Q and Zhang J. Pyroptosis: a new regulating mechanism in cardiovascular disease. J Inflamm Res 2021; 14: 2647-2666.
[20] Kang J, Jia Z, Ping Y, Liu Z, Yan X, Xing G and Yan W. Testosterone alleviates mitochondrial ROS accumulation and mitochondria-mediated apoptosis in the gastric mucosa of orchiectomized rats. Arch Biochem Biophys 2018; 649: 53-59.
[21] Liu H, Chen Y, Hu Y, Zhang W, Zhang H, Su T, Wang J, Yin Z, Zhao X, Zhou X, Li L, Zou Y, Fu Y, Zhang Y and Song X. Protective effects of an alcoholic extract of Kaempferia galanga L. rhizome on ethanol-induced gastric ulcer in mice. J Ethnopharmacol 2024; 325: 117845.
[22] Yang Y, Du J, Liu F, Wang X, Li X and Li Y. Role of caspase-3/E-cadherin in helicobacter pylori-induced apoptosis of gastric epithelial cells. Oncotarget 2017; 8: 59204-59216
[23] Wu Y, Hu J, Long X, Pan Y, Mu J, Park KY and Zhao X. *Lactobacillus plantarum* ZS62 alleviates alcohol-induced gastric injury in mice via an anti-oxidative mechanism. Drug Des Devel Ther 2021; 15: 1667-1676.
[24] Ardalani H, Hadipanah A and Sahebkar A. Medicinal plants in the treatment of peptic ulcer disease: a review. Mini Rev Med Chem 2020; 20: 662-702.
[25] Tang D, Zhang Q, Duan H, Ye X, Liu J, Peng W and Wu C. Polydatin: a critical promising natural agent for liver protection via antioxidative stress. Oxid Med Cell Longev 2022; 2022: 9218738.
[26] Gündoğdu AÇ, Özbayer C and Kar F. Boric acid alleviates gastric ulcer by regulating oxidative stress and inflammation-related multiple signaling pathways. Biol Trace Elem Res 2024; 202: 2124-2132.
[27] Diesinger T, Buko V, Lautwein A, Dvorsky R, Belonovskaya E, Lukivskaya O, Naruta E, Kirko S, Andreev V, Buckert D, Bergler S, Renz C, Schneider E, Kuchenbauer F, Kumar M, Günes C, Büchele B, Simmet T, Müller-Enoch D, Wirth T and Haehner T. Drug targeting CYP2E1 for the treatment of early-stage alcoholic steatohepatitis. PLoS One 2020; 15: e0235990.
[28] Park CH, Son HU, Yoo CY and Lee SH. Low molecular-weight gel fraction of Aloe vera exhibits gastroprotection by inducing matrix metalloproteinase-9 inhibitory activity in alcohol-induced acute gastric lesion tissues. Pharm Biol 2017; 55: 2110-2115.
[29] Birngruber CG, Holz F and Verhoff MA. Letter to the editor regarding "Undetected traumatic diastasis of cranial sutures in a case of

child abuse". Forensic Sci Int 2019; 304: 10-9954.
[30] Kan J, Hood M, Burns C, Scholten J, Chuang J, Tian F, Pan X, Du J and Gui M. A novel combination of wheat peptides and fucoidan attenuates ethanol-induced gastric mucosal damage through anti-oxidant, anti-inflammatory, and pro-survival mechanisms. Nutrients 2017; 9: 978.
[31] Ermis A, Aritici Colak G, Acikel-Elmas M, Arbak S and Kolgazi M. Ferulic acid treats gastric ulcer via suppressing oxidative stress and inflammation. Life 2023; 13: 388.
[32] Çakır Gündoğdu A, Kar F and Özbayer C. Investigation of the gastroprotective effect of betaine-homocysteine homeostasis on oxidative stress, inflammation and apoptosis in ethanol-induced ulcer model. J Invest Surg 2022; 35: 1806-1817.
[33] Cheng H and An X. Cold stimuli, hot topic: an updated review on the biological activity of menthol in relation to inflammation. Front Immunol 2022; 13: 1023746.
[34] Liu F, Nong X, Qu W and Li X. Weikangling capsules combined with omeprazole ameliorates ethanol-induced chronic gastritis by regulating gut microbiota and EGF-EGFR-ERK pathway. Life Sci 2023; 315: 121368.
[35] Takeuchi K and Amagase K. Roles of cyclooxygenase, prostaglandin E2 and ep receptors in mucosal protection and ulcer healing in the gastrointestinal tract. Curr Pharm Des 2018; 24: 2002-2011.
[36] Wu RM, Pei ZJ, Zhang HQ, Gao Y and Duan XY. Effects of miR-362 in regulating the proliferation, invasion and apoptosis of gastric cancer by inhibiting the expression of tumor-promoting factor PRDM2. Crit Rev Eukaryot Gene Expr 2021; 31: 11-21.
[37] He Q, Liu M, Rong Z, Liang H, Xu X, Sun S, Lei Y, Li P, Meng H, Zheng R, Bi Y, Chen X, Wang B, Zhao J and Jiang K. Rebamipide attenuates alcohol-induced gastric epithelial cell injury by inhibiting endoplasmic reticulum stress and activating autophagy-related proteins. Eur J Pharmacol 2022; 922: 174891.
[38] Wu Y, Duan Z, Qu L, Zhang Y, Zhu C and Fan D. Gastroprotective effects of ginsenoside Rh4 against ethanol-induced gastric mucosal injury by inhibiting the MAPK/NF-κB signaling pathway. Food Funct 2023; 14: 5167-5181.